Refined one-dimensional models for the multi-field analysis of layered smart structures

Refined one-dimensional models for the multi-field analysis of layered smart structures

Enrico Zappino and Erasmo Carrera

Abstract The analysis of layered structures requires the use of numerical tools that able to describe the complex behavior that can appear at the interface between two different materials. The use of the Finite Element Method can only lead to accurate results if the kinematic assumptions of the structural models allow complex deformation fields to be evaluated, and as a consequence classical models are often ineffective in the analysis of such structures. The use of the Carrera Unified Formulation provides a general tool that can be used to derive refined one-dimensional models in a compact form. The use of a refined kinematic description over the cross-section of an element leads to accurate results even when multi-field problems are considered, that is when complex stress fields appear. A comprehensive derivation of a class of refined one-dimensional models, which are able to deal with multi-layer structures and multi-field problems, is presented in this section. Thermal and piezoelectric effects are considered, and a fully coupled thermo-piezo-elastic model is presented. Finally, some benchmarks are shown in order to verify the accuracy of the presented models

1 Introduction

The development of innovative structures requires the use of numerical tools that are able to deal with the complexities introduced by innovative materials. Laminated materials are used extensively in all engineering fields, and they can appear in many different forms. The most common layered structures are made up of composite

Enrico Zappino
Mul^2*Team*, Politecnico di Torino, Corso Duca dgli Abruzzi 24, Torino, Italy e-mail: enrico.zappino@polito.it

Erasmo Carrera
Mul^2*Team*, Politecnico di Torino, Corso Duca dgli Abruzzi 24, Torino, Italy e-mail: ersmo.carrera@polito.it

materials, see Fig. 1a, that exploit the orthotropic properties of the fiber reinforced layers to increase the stiffness of the structural component in the desired direction. When the weight of the structure is one of the design parameters, the use of sandwich materials, see Fig. 1b, may lead to an improvement in the bending resistance without increasing the total weight of the structure. Sandwich materials exploit a thick soft core and two external skins. The core, in addition to absorbing the shear load, increases the distance of the skins from the neutral axis. Another example of

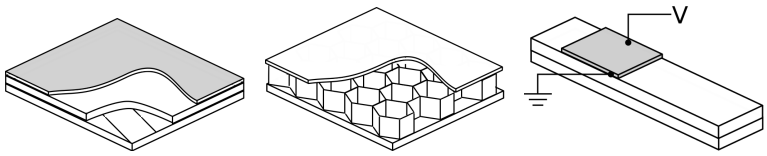

(a) Composite Material (b) Sandwich Material (c) Piezo-layered beam

Fig. 1 Examples of layered structures.

layered material is that used in smart structures, see Fig. 1c. In this case, a layer or a patch of active material, e.g. piezoelectric material, is bonded onto a structure with the purpose of exploiting the piezo-elastic effect as an actuator or a sensor. Piezo-layered structures have become very important over the last few decades because they are at the basis of the development of MEMS (Micro Electro-Mechanical Systems) devices. The present work has focused on piezo-layered structures, although it is common to find piezoelectric patches on composite materials and sandwich panels.

The analysis of layered beam structures involves evaluating complex stress fields. When the Euler-Bernoulli [31] beam model is used, it is accepted that the solution can only be considered accurate for slender bodies and isotropic materials, that is, it cannot be applied to layered structures. If moderately stubby structures are considered the model proposed by Timoshenko [50] has to be used to include shear effects, and in this case, the use of a shear correction factor, see [50, 25, 29], is required to overcome the approximation of a constant shear distribution over the cross-section. Even though the Timoshenko model is more accurate than the Euler-Bernoulli theory, neither of these classical models is suitable for the stress analysis of layered structures because they are not able to properly describe the layers interfaces. The introduction of refined structural models allows the limitations introduced by the fundamental assumptions of the classical models to be overcome and the stress singularities due to local effects to be dealt with. Carrera, see [7], pointed out that the analysis of layered structures requires a numerical model that is able to fulfill the C_z^0 requirement, that is, the continuity of the transversal stress component has to be ensured to obtain reliable results.

Many refined one-dimensional models have been proposed over the last few decades, e.g. the use of warping functions, as proposed by Vlasov [54], which allows the cross-section deformation to be included in beam models. Cross-sectional

warping plays an essential role in thin-walled structures, as shown in the work by Friberg [32] and Ambrosini [2], where the warping function approach was used. Schardt [47] proposed a one-dimensional model for the thin-walled structures analysis where the displacement field was considered as an expansion around the mid-plane of the thin-walled cross-section. This approach, which is called the generalized beam theory (GBT), was also used by Davies and Leach [27] and Davies *et al.*[28], and an extension to the analysis of composite material was proposed by Silvestre and Camotim [48]. The Variation Asymptotic Method, VAM, proposed by Berdichevsky [5], uses a characteristic cross-section parameter to build an asymptotic expansion of the solution. The application of this approach to one-dimensional structures can be seen in the work by Giavotto *et al.* [33]. Volovoi [55], Yu *et al.* [59] and Yu and Hodges [58] have extended this method to composite materials and beams with arbitrary cross-sections.

All these methods allow the accuracy of one-dimensional models to be improved. The development of these models has been crucial in the design of innovative structures that make use of innovative materials. One of these applications is the development of piezoelectric devices. Fig 2 shows how the analysis of a piezo-layered

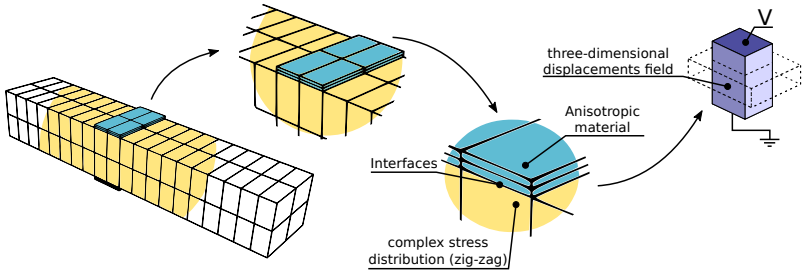

Fig. 2 Example of a piezo-layered structure.

structure requires many aspects to be take into account, such as the material interfaces and the orthotropy of the material. The piezoelectric effect has been known since the 19^{th} century, when the Curie brothers first noticed it. This effect pertains to the conversion of mechanical to electrical energy and vice-versa. The use of piezoelectric materials in structural design is very interesting because of their properties, and a great deal of effort has been made to include the piezoelectric contribution in structural models. Crawley and Luis [26] and Bailey and Hubbard [3] considered the piezoelectric contribution as an additional strain which had to be added to the inactive structure. Classical structural models were used extensively to analyze piezoelectric materials; as shown by Sarvanos and Heyliger [46] in their review. In the past, classical three-dimensional ([30, 57]), two-dimensional ([35, 42]) and one-dimensional models were used to study structures with piezoelectric effects. The use of refined structural models improves the accuracy of the stress and strain fields, especially when complex structures, such as multi-layered structures, are considered. A great deal of effort has been focused on the extension of these models to the

analysis of piezoelectric materials. One of the most critical points is the interface between the structure and piezoelectric patches, as shown by Zhou and Tiersten[64]. The introduction of shear effects, see [24, 37, 38, 39, 52], makes it possible to have a more accurate description of the stress field of the problem. More refined approaches have been proposed in the last few years, see [63, 41, 53]; in these cases, a first order theory has been considered. Carrera [8],Robaldo *et al.* [44] and Carrera *et al.* [12] proposed the use of refined two-dimensional models for the analysis of multi-layered structures, including piezoelectric materials. The use of a refined model over the whole structural domain requires more computational costs than those necessary. The best solution would be to use refined models only in the region in which they are required and classical models elsewhere. The problem of mixing or joining different structural models is a well-known topic in literature as shown by Kim *et al.* [34]. Biscani *et al.* [6] proposed an approach that is able to increase the accuracy of the model, but only where the piezoelectric elements are located. The coupling between of piezo-ceramic and metallic materials can be an problematic when the device has to operate at high temperatures. The large difference between the thermal expansion coefficients (CTE) could lead to large deformations, which in turn could overcome the stroke of the actuator. Accurate numerical models may be used to predict the behavior of these devices, and they can be used in the design process. The use of classical beam models for the thermo-piezo-elastic analysis of multilayer structures can be found in the work by Tzou and Ye [51] and Ahmad *et al.* [1]. Carrera and Robaldo [22] presented a class of refined two-dimensional models for the accurate analysis of plates and shells including thermal and piezoelectric effects.

A unified approach to the development of refined one-dimensional models, which is suitable for multi-field analyses is presented in the following pages. The structural model is based on the Carrera Unified Formulation (CUF), a numerical tool that can be used to derive any order of structural model in a compact and unified form. CUF was firstly developed for two-dimensional models by Carrera [10] and was extended to the thermal-elastic problem by Carrera [9] and Robaldo *et al.* [43]. The piezo-elastic formulation was introduced by Robaldo *et al.* [44]. The fully coupled piezo-thermo-mechanical expansion of the CUF was presented by Carrera and Boscolo [11]. This numerical approach was extended to the one-dimensional model by Carrera *et al.* [18, 20, 21, 23],more details can be found in the books by Carrera *et al.*[14, 17].

The displacement field above the cross-section was described in the work by Carrera and Petrolo [19] through the use of Lagrange-type polynomials. The extension of this model to a multi-field analysis was presented by Miglioretti *et al.*[40] for the piezo-mechanical problem, and was used by Zappino *et al.* [60].

2 Thermo-piezo-elastic one-dimensional model

This section presents the refined one-dimensional model used in the following analyses. The coordinate reference frame is shown in Fig. 3. The displacement three-

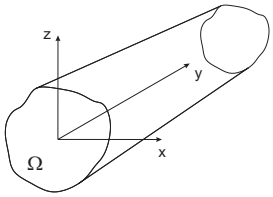

Fig. 3 Beam reference system.

dimensional field is described using the vector $\boldsymbol{u}$:

$$\boldsymbol{u}^T = \left\{u_x,\, u_y,\, u_z\right\} \tag{1}$$

In the thermo-piezo-elastic formulation, in addition to the mechanical variables, also the temperature variation, ϑ, and the electric potential, ϕ, must be considered. The solution of the thermo-piezo-elastic problem requires to define five quantities in each point:

$$\boldsymbol{u}^T = \left\{u_x,\, u_y,\, u_z,\, \vartheta,\, \phi\right\} \tag{2}$$

where vector $\boldsymbol{u}$ contains the unknown quantities.

2.1 Kinematic approximation

The one-dimensional approximation requires to assume a known displacement field, a temperature variation and a electric potential over the cross-section. Different formulation can be used, in the following pages a review of the classical models and the details of the refined kinematic assumptions used in the present work are presented.

2.1.1 Classical beam models

Classical beam models are subject to a number of fundamental assumptions that limit the use of these models to a small number of applications.

The Euler-Bernoulli beam theory, EBBT, does not consider shear effects and the warping of the cross-section, which is considered rigid in- and out-of-plane. The displacement field of the cross-section can be written as:

$$\begin{aligned} u_x &= u_{x_1} \\ u_y &= u_{y_1} + x\,\frac{\partial u_{z_1}}{\partial y} + z\,\frac{\partial u_{x_1}}{\partial y} \\ u_z &= u_{z_1} \end{aligned} \tag{3}$$

This model has only three degrees of freedom, DOF, over the cross-section because the rotation of the cross-section is considered as the derivatives of the rigid translation.

The Timoshenko beam theory, TBT, includes the effects of the shear but it is considered constant over the cross-section. In this case, the displacement field of the cross-section can be written as:

$$\begin{aligned} u_x &= u_{x_1} \\ u_y &= u_{y_1} + x\,u_{y_2} + z\,u_{y_3} \\ u_z &= u_{z_1} \end{aligned} \tag{4}$$

The TBT has five DOFs, because the cross-sectional rotation is a free parameter. The use of these models is limited to slender (EBBT) and moderately slender (TBT) bodies, because the fundamental assumptions are only verified for these geometries. In the present form these models can be used to describe the bending of prismatic beam. The torsional effects can be included considering the contributions introduced by [45] or, in the case of thin-walled structures, by [54].

The use of refined one-dimensional models allows the range of applicability of these models to be extended to a large number of applications. In this work the refined one-dimensional models derived from using the CUF are used to build node-dependent kinematic one-dimensional models. A brief review of these models is presented in the following section.

2.1.2 Refined one-dimensional models

The one-dimensional approximation requires a known displacement field to be assumed over the cross-section. A function expansion can be used to describe properly the behavior of the beam cross-section. This approach, suggest by [56], leads to write the three-dimensional displacement field as:

$$\boldsymbol{u} = \boldsymbol{u}_\tau(y) F_\tau(x,z), \qquad \tau = 1 \ldots M. \tag{5}$$

where $F_\tau(x,z)$ is the function expansion over the cross-section, $\boldsymbol{u}_\tau(y)$ is the unknown vector along the beam axis, and M is the number of terms in the functions expansion $F_\tau(x,z)$. The choice of the functions expansion allows the kinematic of the model to be modified. A number of possible choices were presented by [16]. In the present work Taylor and Lagrange expansions are considered, more details are reported in the next sections.

The displacements approximation introduced in Eq.5 leads to a one-dimensional problem. The solution of this problem can be obtained using the Finite Element Method, FEM, which allows the system of partial derivative functions to be reduced to an algebraic system. FEM approximates the axial unknowns $\boldsymbol{u}_\tau(y)$ using the one-dimensional shape functions N_i, that is, the displacement field assumes the formulation:

$$\boldsymbol{u} = \boldsymbol{u}_{i\tau} N_i(y) F_\tau(x,z), \qquad \tau = 1 \dots M; \qquad i = 1 \dots N_n. \tag{6}$$

where N_i are the shape functions introduced by the FE model, N_n is the number of nodes of the element and $\boldsymbol{u}_{i\tau}$ are the nodal unknowns. The variation of the displacement can be written as:

$$\delta\boldsymbol{u} = \delta\boldsymbol{u}_{js} N_j(y) F_s(x,z), \qquad s = 1 \dots M; \qquad j = 1 \dots N_n. \tag{7}$$

2.1.3 Taylor expansion models (TE)

The one-dimensional TE model consists of an expansion that uses 2D polynomials $x^m z^n$, as F_τ, where m and n are positive integers. For instance, the second-order displacement field is:

$$\begin{aligned} u_x &= u_{x_1} + x\, u_{x_2} + z\, u_{x_3} + x^2\, u_{x_4} + xz\, u_{x_5} + z^2\, u_{x_6} \\ u_y &= u_{y_1} + x\, u_{y_2} + z\, u_{y_3} + x^2\, u_{y_4} + xz\, u_{y_5} + z^2\, u_{y_6} \\ u_z &= u_{z_1} + x\, u_{z_2} + z\, u_{z_3} + x^2\, u_{z_4} + xz\, u_{z_5} + z^2\, u_{z_6} \end{aligned} \tag{8}$$

Figure 4 shows a representation of a two nodes element based on the TE expansion.

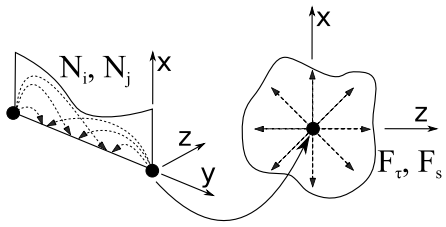

Fig. 4 A two-nodes beam based on the Taylor expansion.

In this case, the F_τ and F_s functions are used to expand the solution from the beam node to the cross-section.

2.1.4 Lagrange expansion models (LE)

In the case of LE models, Lagrange polynomials are used to build refined one-dimensional models. The iso-parametric formulation is exploited to deal with arbi-

trary cross-section shaped geometries. For instance, the linear interpolation functions are:

$$F_1 = \frac{1}{4}(1-\xi)(1-\eta);\ F_2 = \frac{1}{4}(1+\xi)(1-\eta);$$
$$F_3 = \frac{1}{4}(1+\xi)(1+\eta);\ F_4 = \frac{1}{4}(1-\xi)(1+\eta) \tag{9}$$

where ξ and η are the coordinates in the natural reference system. Equation 9 coincides with the linear Lagrange polynomial in two dimensions. In this paper a quadratic element with nine nodes, LE9, is used. When LE is used the unknowns are only the displacements of the cross-sectional nodes.

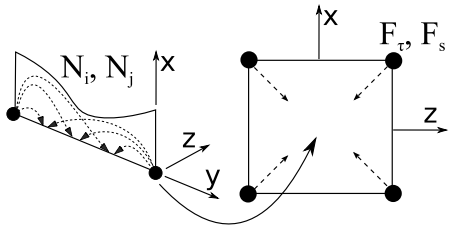

Fig. 5 A two-nodes beam based on the Lagrange expansion.

Figure 5 shows a representation of a two nodes element based on the LE. In this case the F_τ and F_s functions are used to expand the solution from the cross-sectional nodes to the cross-section area.

This approach is very effective when layered structure are considered. Fig. 6 shows a layered beam, the beam has two layer but there is a patch at one end, that is, in that area three layer are present. Fig. 6 shows how each layer can be represented

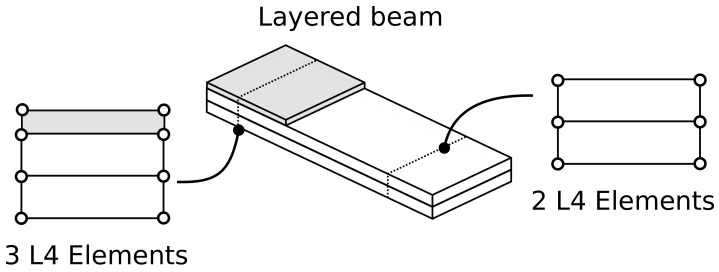

Fig. 6 Example of the cross-sectional discretization of a layered structure.

with a different element over the cross section. This approach allow the accuracy of the results to be increased because a *zig-zag* displacement field can be predicted.

2.2 Geometrical relations

The geometrical relations in the case of the thermo-piezo-elastic model allow the strain ($\boldsymbol{\varepsilon}$), the spatial thermal variations (θ) and the electric field ($\boldsymbol{E}$) to be evaluated. The strain vector, $\boldsymbol{\varepsilon}$, can be written as:

$$\boldsymbol{\varepsilon} = \{\varepsilon_{xx}\ \varepsilon_{yy}\ \varepsilon_{zz}\ \varepsilon_{xz}\ \varepsilon_{yz}\ \varepsilon_{xy}\ \}^T = \boldsymbol{D}_u \boldsymbol{u} \tag{10}$$

where $\boldsymbol{D}_u$ is:

$$\boldsymbol{D}_u^T = \begin{bmatrix} \partial_x & 0 & 0 & \partial_z & 0 & \partial_y \\ 0 & \partial_y & 0 & 0 & \partial_z & \partial_x \\ 0 & 0 & \partial_z & \partial_x & \partial_y & 0 \end{bmatrix} \tag{11}$$

The spatial temperature variation, $\boldsymbol{\theta}$, can be written as:

$$\boldsymbol{\theta} = \left\{ \frac{\partial \vartheta}{\partial x}\ \frac{\partial \vartheta}{\partial y}\ \frac{\partial \vartheta}{\partial z} \right\}^T = \boldsymbol{D}_\vartheta\, \vartheta \tag{12}$$

where $\boldsymbol{D}_\vartheta$ is:

$$\boldsymbol{D}_\vartheta = \left\{ \partial_x\ \partial_y\ \partial_z \right\}^T \tag{13}$$

The electric field, $\boldsymbol{E}$, can be expressed as:

$$\boldsymbol{E} = \left\{ \frac{\partial \phi}{\partial x}\ \frac{\partial \phi}{\partial y}\ \frac{\partial \phi}{\partial z} \right\}^T = \boldsymbol{D}_\phi\, \phi \tag{14}$$

where $\boldsymbol{D}_\phi$ is equal to $\boldsymbol{D}_\vartheta$. The symbol ∂ stands for partial derivative, that is: $\partial_x = \frac{\partial}{\partial x}$, $\partial_y = \frac{\partial}{\partial y}$ and $\partial_z = \frac{\partial}{\partial z}$

2.3 Constitutive relations

The constitutive equation for the thermo-piezo-elastic model have been derived in according with the work presented by Carrera *et al.*[13].

The stress, $\boldsymbol{\sigma}$ can be written in the following form:

$$\boldsymbol{\sigma} = \boldsymbol{C}\boldsymbol{\varepsilon} - \boldsymbol{\lambda}\,\vartheta - \boldsymbol{e}\boldsymbol{E} \tag{15}$$

The first contribution comes from the Hook's law and derives from the mechanical problem.

$$\begin{Bmatrix} \sigma_{xx} \\ \sigma_{yy} \\ \sigma_{zz} \\ \sigma_{xz} \\ \sigma_{yz} \\ \sigma_{xy} \end{Bmatrix} = \begin{bmatrix} C_{11} & C_{12} & C_{13} & 0 & 0 & C_{16} \\ C_{21} & C_{22} & C_{23} & 0 & 0 & C_{26} \\ C_{31} & C_{32} & C_{33} & 0 & 0 & C_{36} \\ 0 & 0 & 0 & C_{44} & C_{45} & 0 \\ 0 & 0 & 0 & C_{54} & C_{55} & 0 \\ C_{61} & C_{62} & C_{63} & 0 & 0 & C_{66} \end{bmatrix} \begin{Bmatrix} \varepsilon_{xx} \\ \varepsilon_{yy} \\ \varepsilon_{zz} \\ \varepsilon_{xz} \\ \varepsilon_{yz} \\ \varepsilon_{xy} \end{Bmatrix} \tag{16}$$

The second therm, $\boldsymbol{\lambda}\vartheta$, comes from the thermo-mechanical coupling. The vector $\boldsymbol{\lambda}$ can be written as:

$$\boldsymbol{\lambda} = \boldsymbol{C}\alpha = \boldsymbol{C}\{\alpha_1 \ \alpha_2 \ \alpha_3 \ 0 \ 0 \ 0 \ \}^T \tag{17}$$

Where $\boldsymbol{C}$ is the matrix with the elastic coefficients of the material, and α is the vector of the thermal expansion coefficients. The last term, $\boldsymbol{eE}$, comes from the electro-mechanical coupling. The matrix $\boldsymbol{e}$ contains the piezoelectric stiffness coefficients and can be written as:

$$\boldsymbol{e} = \boldsymbol{C}d = \boldsymbol{C}\begin{bmatrix} 0 & 0 & 0 & 0 & d_{15} & 0 \\ 0 & 0 & 0 & d_{24} & 0 & 0 \\ d_{31} & d_{32} & d_{33} & 0 & 0 & 0 \end{bmatrix}^T \tag{18}$$

where d is the matrix of the piezoelectric coefficients.

The electric displacement, $\boldsymbol{D}$, can be written in the following form:

$$\boldsymbol{D} = \boldsymbol{e\varepsilon} + \boldsymbol{\chi E} + \boldsymbol{p}\vartheta \tag{19}$$

The first term, $\boldsymbol{e\varepsilon}$, comes from the electro-mechanical coupling. The second contribution, $\boldsymbol{\chi E}$, is due to the electric problem, $\boldsymbol{\chi}$ is to the dielectric permittivity matrix of the material:

$$\boldsymbol{\chi} = \begin{bmatrix} \chi_{11} & \chi_{12} & 0 \\ \chi_{21} & \chi_{22} & 0 \\ 0 & 0 & \chi_{33} \end{bmatrix} \tag{20}$$

The last term, $\boldsymbol{p}\vartheta$, comes from the thermo-electric problem and $\boldsymbol{p}$ is the vector of the pyro-electric coefficients.

The last constitutive equation describe the heat flux, $\boldsymbol{h}$:

$$\boldsymbol{h} = \boldsymbol{\kappa\theta} \tag{21}$$

where $\boldsymbol{\kappa}$ is the conductivity coefficients matrix:

$$\boldsymbol{\kappa} = \begin{bmatrix} \kappa_{11} & \kappa_{12} & 0 \\ \kappa_{21} & \kappa_{22} & 0 \\ 0 & 0 & \kappa_{33} \end{bmatrix} \tag{22}$$

2.4 Governing equation

The governing equation can be written using the virtual displacements principle, PVD:

$$\delta L_{int} = \delta L_{ext} \tag{23}$$

where δL_{int} is the variation of the internal work while, δL_{ext} is the variation of the external work.

In explicit form the PVD can be written as:

$$\delta L_{int} = \int_V (\delta \boldsymbol{\varepsilon}^T \boldsymbol{\sigma} - \delta \boldsymbol{\theta}^T \boldsymbol{h} - \delta \boldsymbol{E}^T \boldsymbol{D}) dV = \delta L_{ext} \tag{24}$$

If geometrical and constitutive equation are substituted in Equation 24 the following equation is obtained:

$$\begin{aligned} \delta L_{int} = \int_V (&\delta \boldsymbol{\varepsilon}^T \boldsymbol{C} \boldsymbol{\varepsilon} - \delta \boldsymbol{\varepsilon}^T \boldsymbol{\lambda} \vartheta - \delta \boldsymbol{\varepsilon}^T \boldsymbol{e} \boldsymbol{E} + \delta \boldsymbol{\theta}^T \boldsymbol{\kappa} \boldsymbol{\theta} + \\ &- \delta \boldsymbol{E}^T \boldsymbol{e} \boldsymbol{\varepsilon} - \delta \boldsymbol{E}^T \boldsymbol{\chi} \boldsymbol{E} - \delta \boldsymbol{E}^T \boldsymbol{p} \vartheta) dV \end{aligned} \tag{25}$$

If the kinematic approximation introduced before is used the terms that compose the variation of the internal work can be written in matrix form.

The first term, $\delta \boldsymbol{\varepsilon}^T \boldsymbol{C} \boldsymbol{\varepsilon}$, represents the mechanical problem. The strain can be expressed in therm of derivatives of the displacements, moreover the displacements can be written using the shape functions N_i and F_τ.

$$\begin{aligned} \int_V \delta \boldsymbol{\varepsilon}^T \boldsymbol{C} \boldsymbol{\varepsilon} dV =& \delta \boldsymbol{q}_{u\,js}^T \int_V N_j F_s \boldsymbol{I} \boldsymbol{D}_u^T \boldsymbol{C} \boldsymbol{D}_u \boldsymbol{I} F_\tau N_i dV \boldsymbol{q}_{ui\tau} = \\ =& \delta \boldsymbol{q}_{u\,js}^T \boldsymbol{k}_{uu}^{ij\tau s} \boldsymbol{q}_{ui\tau} \end{aligned} \tag{26}$$

$\boldsymbol{k}_{uu}^{ij\tau s}$ is the fundamental nucleus of size 3×3 of the stiffness matrix of the pure mechanical problem. $\boldsymbol{q}_{ui\tau}$ is the part of the unknown vector related to the mechanical variables.

The term $\delta \boldsymbol{\varepsilon}^T \boldsymbol{\lambda} \vartheta$ can be written as:

$$\begin{aligned} \int_V \delta \boldsymbol{\varepsilon}^T \boldsymbol{\lambda} \vartheta dV =& \delta \boldsymbol{q}_{u\,js}^T \int_V N_j F_s \boldsymbol{I} \boldsymbol{D}_u^T \boldsymbol{\lambda} \boldsymbol{I} F_\tau N_i dV \boldsymbol{q}_{\vartheta\, i\tau} = \\ =& \delta \boldsymbol{q}_{u\,js}^T \boldsymbol{k}_{u\theta}^{ij\tau s} \boldsymbol{q}_{ui\tau} \end{aligned} \tag{27}$$

$\boldsymbol{k}_{u\theta}^{ij\tau s}$ is the fundamental nucleus of size 3×1 of the stiffness matrix of the thermo-elastic problem. $\boldsymbol{q}_{\vartheta\, i\tau}$ is the part of the unknown vector related to the thermal variable.

The term $\delta \boldsymbol{\varepsilon}^T \boldsymbol{e} \boldsymbol{E}$ can be written as:

$$\begin{aligned} \int_V \delta \boldsymbol{\varepsilon}^T \boldsymbol{e} \boldsymbol{E} dV =& \delta \boldsymbol{q}_{u\,js}^T \int_V N_j F_s \boldsymbol{I} \boldsymbol{D}_u^T \boldsymbol{e} \boldsymbol{D}_\phi \boldsymbol{I} F_\tau N_i dV \boldsymbol{q}_{\phi\, i\tau} = \\ =& \delta \boldsymbol{q}_{u\,js}^T \boldsymbol{k}_{u\phi}^{ij\tau s} \boldsymbol{q}_{ui\tau} \end{aligned} \tag{28}$$

$\boldsymbol{k}_{u\phi}^{ij\tau s}$ is the fundamental nucleus of size 3×1 of the stiffness matrix of the piezo-elastic problem. $\boldsymbol{q}_{\phi\, i\tau}$ is the part of the unknown vector related to the electrical variable.

The term $\delta \boldsymbol{\theta}^T \boldsymbol{\kappa} \boldsymbol{\theta}$ can be written as:

$$\begin{aligned} \int_V \delta \boldsymbol{\theta}^T \boldsymbol{\kappa} \boldsymbol{\theta} dV =& \delta \boldsymbol{q}_{\vartheta\,js}^T \int_V N_j F_s \boldsymbol{I} \boldsymbol{D}_\vartheta^T \boldsymbol{\kappa} \boldsymbol{D}_\vartheta \boldsymbol{I} F_\tau N_i dV \boldsymbol{q}_{\vartheta\, i\tau} = \\ =& \delta \boldsymbol{q}_{u\,js}^T \boldsymbol{k}_{\theta\theta}^{ij\tau s} \boldsymbol{q}_{ui\tau} \end{aligned} \tag{29}$$

$\boldsymbol{k}_{\theta\theta}^{ij\tau s}$ is the fundamental nucleus of size 1×1 of the stiffness matrix of the pure thermal problem.

The term $\delta \boldsymbol{E}^T \boldsymbol{e}\boldsymbol{\varepsilon}$ can be written as:

$$\begin{aligned}\int_V \delta \boldsymbol{E}^T \boldsymbol{e}\boldsymbol{\varepsilon} dV =& \delta {\boldsymbol{q}_\phi}_{js}^T \int_V N_j F_s I \boldsymbol{D}_\phi^T \boldsymbol{e} \boldsymbol{D}_u I F_\tau N_i dV \boldsymbol{q}_{ui\tau} = \\ =& \delta {\boldsymbol{q}_\phi}_{js}^T \boldsymbol{k}_{\phi u}^{ij\tau s} \boldsymbol{q}_{ui\tau}\end{aligned} \tag{30}$$

$\boldsymbol{k}_{\phi u}^{ij\tau s}$ is the fundamental nucleus of size 1×3 of the stiffness matrix of the piezo-elastic problem.

The term $\delta \boldsymbol{E}^T \boldsymbol{\chi} \boldsymbol{E}$ can be written as:

$$\begin{aligned}\int_V \delta \boldsymbol{E}^T \boldsymbol{\chi} \boldsymbol{E} dV =& \delta {\boldsymbol{q}_\phi}_{js}^T \int_V N_j F_s I \boldsymbol{D}_\phi^T \boldsymbol{\chi} \boldsymbol{D}_\phi I F_\tau N_i dV \boldsymbol{q}_{\phi i\tau} = \\ =& \delta {\boldsymbol{q}_\phi}_{js}^T \boldsymbol{k}_{\phi\phi}^{ij\tau s} \phi_{i\tau}\end{aligned} \tag{31}$$

$\boldsymbol{k}_{\phi\phi}^{ij\tau s}$ is the fundamental nucleus of size 1×1 of the stiffness matrix of the pure electric problem.

The term $\delta \boldsymbol{E}^T \boldsymbol{p} \vartheta$ can be written as:

$$\begin{aligned}\int_V \delta \boldsymbol{E}^T \boldsymbol{p} \vartheta dV =& \delta {\boldsymbol{q}_\phi}_{js}^T \int_V N_j F_s I \boldsymbol{D}_\phi^T \boldsymbol{p} I F_\tau N_i dV \boldsymbol{q}_{\theta i\tau} = \\ =& \delta {\boldsymbol{q}_\phi}_{js}^T \boldsymbol{k}_{\phi\theta}^{ij\tau s} \theta_{i\tau}\end{aligned} \tag{32}$$

$\boldsymbol{k}_{\phi\theta}^{ij\tau s}$ is the fundamental nucleus of size 1×1 of the stiffness matrix of the pyro-electric problem.

All the fundamental nucleus can be assembled together in fundamental nucleus of the multi-field problem:

$$\delta L_{int} = \delta \boldsymbol{u}_{js}^T \overbrace{\begin{bmatrix} \begin{bmatrix} \ddots & & \\ & \boldsymbol{k}_{uu} & \\ & & \ddots \end{bmatrix} & \begin{bmatrix} \vdots \\ \boldsymbol{k}_{u\theta} \\ \vdots \end{bmatrix} & \begin{bmatrix} \vdots \\ \boldsymbol{k}_{u\phi} \\ \vdots \end{bmatrix} \\ \begin{bmatrix} \cdots & 0 & \cdots \end{bmatrix} & \begin{bmatrix} \boldsymbol{k}_{\theta\theta} \end{bmatrix} & \begin{bmatrix} 0 \end{bmatrix} \\ \begin{bmatrix} \cdots & \boldsymbol{k}_{\phi u} & \cdots \end{bmatrix} & \begin{bmatrix} \boldsymbol{k}_{\phi\theta} \end{bmatrix} & \begin{bmatrix} \boldsymbol{k}_{\phi\phi} \end{bmatrix} \end{bmatrix}}^{k^{ij\tau s}} \boldsymbol{u}_{i\tau} \tag{33}$$

The contributions $\boldsymbol{k}_{\theta\phi}$ and $\boldsymbol{k}_{\theta u}$ can be neglected when an external temperature is imposed as boundary condition, as in the present paper. As can be seen in Eq. 33, when the multi-field case is considered the nucleus is no more symmetric, as a consequence the global stiffness matrix loses the properties that come from the sym-

metry, this can reduce the efficiency of the numerical solution and an appropriate solver must be used.

2.5 Loading Vector

The virtual work due to the load $\boldsymbol{P} = \{P_x, P_y, P_z, P_\theta, P_\phi\}$ can be expressed as:

$$\delta L_{ext} = \int_V \delta \boldsymbol{u}^T \boldsymbol{P} dV \tag{34}$$

Considering the displacement function the external work can be written as:

$$\delta L_{ext} = \delta \boldsymbol{u}_{sj}^T \int_V F_s^j N_j \boldsymbol{P} dV = \delta \boldsymbol{u}_{sj}^T \cdot \boldsymbol{p}_{sj} \tag{35}$$

where $\boldsymbol{p}_{sj}$ is the expression of the fundamental nucleus of the load vector.

2.6 Rotation and assembly of the fundamental nucleus

The analysis of complex structures requires finite elements to be rotated in any direction and the stiffness to be computed in a given reference system, that is, the displacements have to be expressed in the same, global reference system. The matrices can be written in the global reference system using a rotation matrix, with respect to the local reference system. The rotation matrices are:

$$\boldsymbol{\Lambda_x} = \begin{bmatrix} 1 & 0 & 0 \\ 0 & cos(\theta) & sin(\theta) \\ 0 & -sin(\theta) & cos(\theta) \end{bmatrix}, \tag{36}$$

$$\boldsymbol{\Lambda_y} = \begin{bmatrix} cos(\phi) & 0 & sin(\phi) \\ 0 & 1 & 0 \\ -sin(\phi) & 0 & cos(\phi) \end{bmatrix}, \tag{37}$$

$$\boldsymbol{\Lambda_z} = \begin{bmatrix} cos(\xi) & -sin(\xi) & 0 \\ sin(\xi) & cos(\xi) & 0 \\ 0 & 0 & 1 \end{bmatrix} \tag{38}$$

where θ, ϕ and ξ are the rotation angles around the x,y,and z axis, as shown in Fig. 7 The displacement vector in the global reference system, $\boldsymbol{u}_{glob}$, can be written as:

$$\boldsymbol{u}_{glob} = \boldsymbol{\Lambda}\boldsymbol{\Lambda_x}\boldsymbol{\Lambda}\boldsymbol{\Lambda_y}\boldsymbol{\Lambda}\boldsymbol{\Lambda_z}\boldsymbol{u}_{loc} = \boldsymbol{\Lambda}\boldsymbol{u}_{loc} \tag{39}$$

Therefore, the mechanical part of the fundamental nucleus in the global reference system becomes:

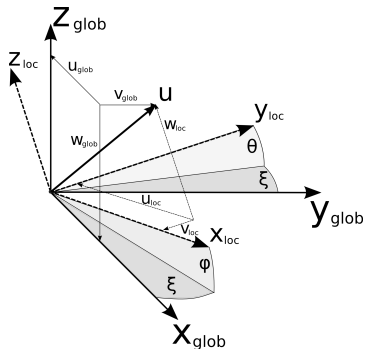

Fig. 7 Representation of the rotation angles.

$$\boldsymbol{k}^{ij\tau s}_{uu_{glob}} = \boldsymbol{\Lambda}^T \boldsymbol{k}^{ij\tau s}_{uu_{loc}} \boldsymbol{\Lambda} \tag{40}$$

The coupling terms can be rotated using the following equations:

$$\boldsymbol{k}^{ij\tau s}_{u\Theta_{glob}} = \boldsymbol{\Lambda}^T \boldsymbol{k}^{ij\tau s}_{u\Theta_{loc}} \tag{41}$$

$$\boldsymbol{k}^{ij\tau s}_{u\phi_{glob}} = \boldsymbol{\Lambda}^T \boldsymbol{k}^{ij\tau s}_{u\phi_{loc}} \tag{42}$$

$$\boldsymbol{k}^{ij\tau s}_{\phi u_{glob}} = \boldsymbol{k}^{ij\tau s^T}_{\phi u_{loc}} \boldsymbol{\Lambda} \tag{43}$$

The terms $\boldsymbol{k}_{\phi\phi}$, $\boldsymbol{k}_{\phi\theta}$ and $\boldsymbol{k}_{\theta\theta}$ are related to scalar fields therefore do not need to be rotated. Once all the elements have been expressed in the same reference system, the global stiffness matrix can be assembled using the classical FEM approach.

2.7 The stiffness matrix assembly

The fundamental nuclei introduced in the previous section, that are discussed extensively in [15], can be used as bricks to build the matrix of the complete structure. Figure 8 shows the procedure used to build the stiffness matrix, starting from the fundamental nucleus.

The loops on τ and s allow to build the stiffness matrix at the node level while the loops on i and j make it possible to create the stiffness matrix at the element level. The assembly on the global stiffness matrix can be done summing the stiffness of the nodes shared by more then one element.

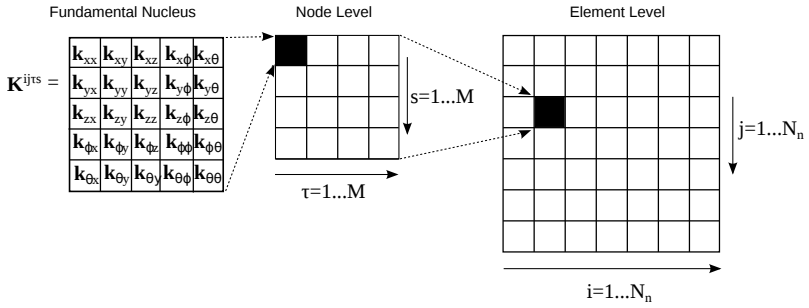

Fig. 8 Stiffness matrix assembly.

3 Numerical Results

The results obtained using the previously introduced structural model are reported in this section. The structural model has been assessed, and the results have been compared with those presented in literature using classical approaches. The Piezo-elastic model has been assessed considering the benchmark proposed by Zhang and Sun [62]. A second case, a beam with piezo-patches, has been considered and the results have been compared with those by [36]. Finally, the results from the thermo-piezo-elastic model have been compared with those by Tzou and Ye [51].

3.1 Piezo-elastic model assessment

A piezo-elastic model has been assessed in this section. The sandwich beam considered in the analysis is shown in Figure 9. The beam has a length, L, of 0.1 m, a thickness of the metallic core, h_c, of 16 mm and two external piezo-patches which have a thickness, h_p, equal to 1 mm. The width is considered equal to 1 m. A potential of 10V is applied to the face of the interface between the piezoelectric patch and the internal core, while, the external free faces have a potential set equal to 0V. The piezoelectric patches are polarized in the z direction.

The properties of the piezoelectric material used in the patches are reported in Table 1, while the properties of the aluminum alloy used in the core are reported in Table 2.

Table 1 Material properties of PZT-5H

C_{11},C_{22},C_{33} [GPa]	C_{12} [GPa]	C_{13},C_{23} [GPa]	C_{44},C_{55},C_{66} [GPa]	e_{15},e_{24} [C/m^2]	e_{31},e_{32} [C/m^2]	e_{33} [C/m^2]	χ_{11},χ_{22} [F/m]	χ_{33} [F/m]
126	79.5	84.1	23.0	17.0	-6.5	23.3	1.503×10^{-8}	1.30×10^{-8}

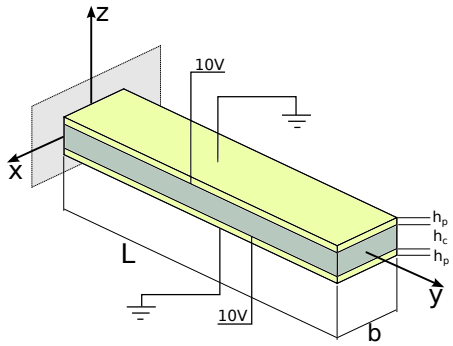

Fig. 9 Geometry of the sandwich beam used in the piezo-elastic assessment

aluminum alloy 1		
Mechanical properties		
E	70.3	GPa
ν	0.345	-

Table 2 aluminum alloy 1 material properties

The displacements due to the applied voltage, have been evaluated. The results have been compared with those of Zhang and Sun [62].

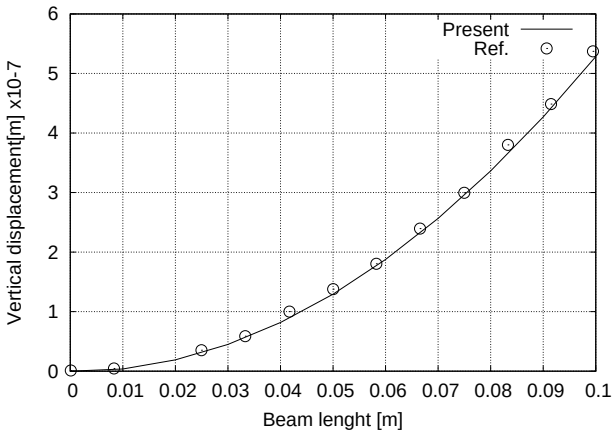

Fig. 10 Vertical displacement of the beam along the y-axis.

Figure 10 shows the vertical displacement of the beam along the length of the beam. The results are in agreement with those presented in literature. This assess-

ment proves that the present beam formulation is able to provide an accurate description of piezo-elastic coupling.

3.2 Cantilever beams with piezo-patches

A cantilevered beam with two piezo-patches has been considered in this section. Benchmark cases of this type have been studied by various researchers such as [49, 61] and [4], as well as [36]. The beam geometry is shown in Fig. 11.

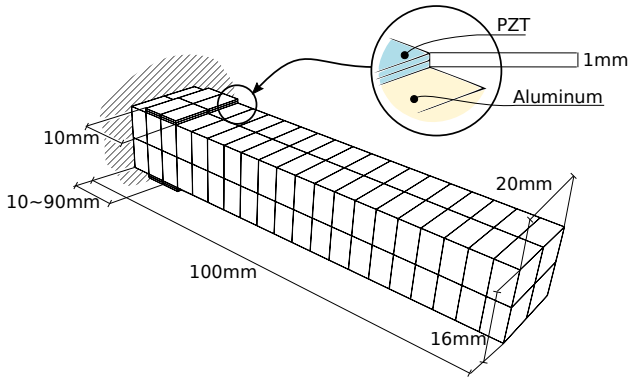

Fig. 11 Geometrical feature of slender beams with piezo-patches

The piezoelectric components are poled in the thickness direction z. A voltage equal to $\Delta\phi = \phi_{bottom} - \phi_{top} = 10$V has been applied for the upper patch and $\Delta\phi = -10$V for the lower one to actuate the beam. The piezoelectric components are made of PZT-5H, whose material coefficients are listed in Table 1, The substrate structures employ aluminum which has the Young modulus $E = 70.3$GPa and a Poisson ratio $\nu = 0.345$. Two cases are considered:

- *Case A*: the piezo-patches cover the whole length of the beam;
- *Case B*: the piezoelectric components have a length $c = 0.01$m and variable positions along the axial direction from $d = 0.01$m to $d = 0.09$m.

The numerical results for *Case A* were obtained with uniform LE nodal kinematics, denoted as "12LE9", which discretizes the cross-section into 12 sub-domains. It should be noted that when Lagrange expansions are adopted to describe the kinematics on a cross-section of a beam, each expansion term possesses specific physical coordinates. The structure is divided into 20 beam elements along the longitudinal direction, and each element has 4 FEM nodes. The obtained results have been compared with the solutions provided by [4] and [36] as well as with those obtained from ABAQUS 3D modelling. The ABAQUS models employ eight layers of C3D20R mechanical brick elements and another eight layers of C3D20RE

piezoelectric brick elements, uniformly distributed 8×40 ($x \times y$) along each layer. The results given by [4] were obtained using a beam element model in which the displacement assumptions were layer-wisely defined (in other words the Bernoulli-Euler theory was used for the faces while the Timoshenko theory was adopted for the cores), and displacement continuity was enforced at the layer interfaces. [36] reached their solution through solid-shell piezoelectric elements, that is, SHB8PSE and SHB20E.

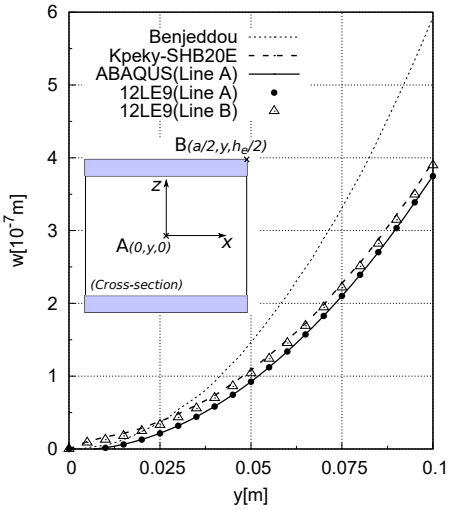

Fig. 12 Vertical displacement along the beam beam, piezo-patches cover the entire length (*Case A*).

The variation in deflection along the beam axis at the central cross-sectional point (lines A) and at one of the upper corners (lines B) are shown in Figure 12 for *Case A*. Table 3.2 compares the deflection on two sets of locations on the free-end cross-sections.

	$w[10^{-7}\text{m}]$	
	$(0,b,0)$	$(\frac{a}{2},b,\frac{h_e}{2})$
ABAQUS	3.749	3.913
12LE9	3.748	3.897

Table 3 Tip deflection of the cantilevered beam in *Case A*

The current solution for the shear configuration in *Case A* shows good agreement with those of [4] and [36].

The models with the same uniform 12LE9 sectional kinematics were also applied to obtain the numerical solutions to *Case B*, and the results are shown in Figure 13.

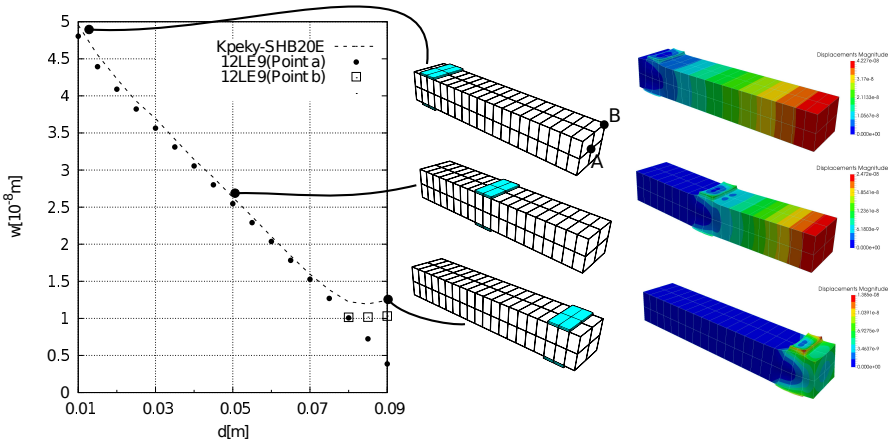

Fig. 13 Tip deflection of the cantilever beams with piezo-patches in *Case B*.

It can be observed that the results based on 12LE9 are in good agreement with the reference solutions taken from literature [36].

A frequency response analysis, in which the patches were closer to the beam root, has been performed using the present model. In this case, the two patches were used as sensors and an external force was applied at the tip of the beam. Fig. 14 shows the frequency response of the cantilevered beam. The dashed line shows the mechanical response, and it can be seen that it identifies the natural frequencies of the structure reported in Tab. 4. The solid line represents the electric response evaluated on the

Natural Frequency	LE Model
1	1363.1
2	1637.2
3	7214.3
4	7460.0
5	8744.9
6	12941.5

Table 4 First six natural frequency of the cantilever beams with piezo-patches

outer surface of the piezo-patch. It can be seen that the resonances of the electric response just appear when the mechanical modes stretch the piezo-patches during the deformation. In the other cases the deformation does not produce an electric response.

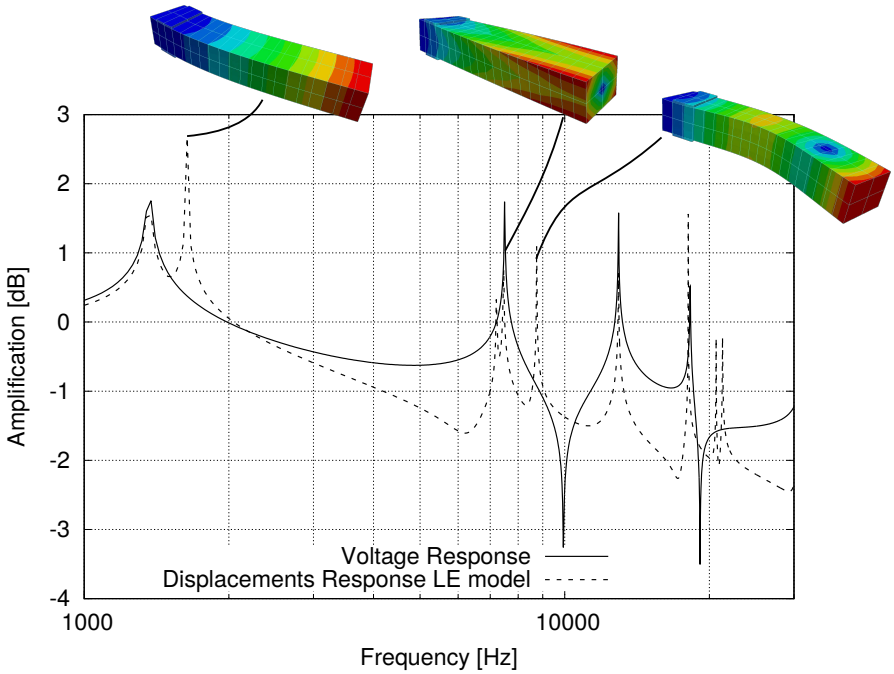

Fig. 14 Frequency response of the cantilever beams with piezo-patches

3.3 Thermo-piezo-elastic model assessment

The fully coupled thermo-piezo-elastic model has been assessed in this section. The structure reported in Figure 16 has been considered. This is once again a sandwich beam but with the following dimensions: L equal to 1 m, b equal to 0.0508 m, the core thickness, h_c, equal to 3.36 mm and the thickness of two external piezo-patches, h_p, equal to 0.254 mm.

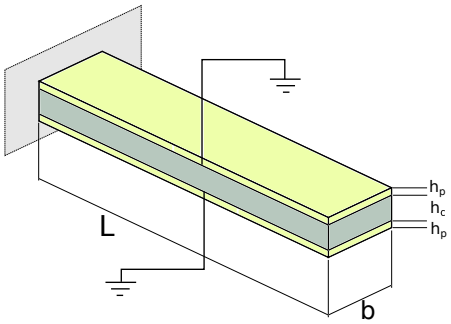

Fig. 15 Geometry of the sandwich beam used in the thermo-piezo-elastic assessment

The internal core has the properties that are reported in Table 5, while the external piezoelectric patches have been built using the same material that was used in the previous assessment, that is PZT-5H. The thermal properties of this material are reported in Table 6.

aluminum alloy 1		
Mechanical properties		
E	68.95	GPa
ν	0.292	-
Thermal properties		
α	11×10^{-6}	$^oC^{-1}$

Table 5 aluminum alloy 2 material properties

PZT-5H		
Thermal properties		
λ_1	2×10^5	$Nm^2\ ^oC^{-1}$
λ_2	2×10^5	$Nm^2\ ^oC^{-1}$
λ_3	-2.7×10^5	$Nm^2\ ^oC^{-1}$
Pyro-electric properties		
p_3	25×10^{-6}	$Cm^2\ ^oC^{-1}$

Table 6 PZT-5H material thermal properties

The structure is subject to a homogeneous thermal environment, that is, at each point the same value of temperature has been imposed. An electric potential of 0V as been considered at the interfaces between the core and the patches, as shown in Figure 16. The voltage of the external layer faces, due to the deformation caused by the thermal load, has been evaluated. The results have been compared with those of Tzou and Ye [51].

Figure 16 shows the variation of the electric potential at different temperatures. It is possible to see that there is a linear correlation between the temperature and the potential. The small difference between the present results and the reference values is due to the different kinematic model that has been adopted. While the reference results were obtained using classical models, the present approach takes into account a *quasi* three-dimensional deformation that produces a slightly higher potential.

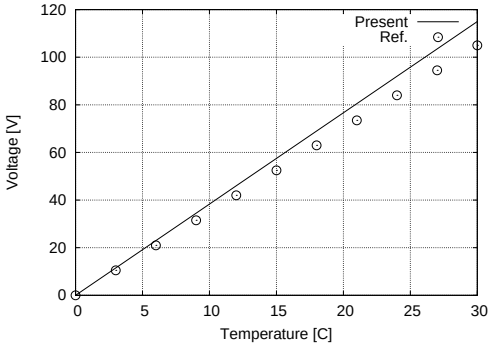

Fig. 16 Upper face potential at different temperature.

4 Conclusions

The multi-field analysis of layered structures requires the use of refined structural models. Finite elements based on a layer-wise approach are able to describe the complex displacement fields due to the variations in the material properties at each layer. In these cases, it is important to have a *zig-zag* capability in the kinematic description, that is, the C_z^0 requirement can be fulfilled. The refined one-dimensional models presented in the present work uses a Lagrange expansion over the cross-section that allows each layer to be described with an independent expansion, or Lagrange element. The computational model has been developed in the framework of the Carrera Unified Formulation, which allows refined structural models to be derived in compact form. The results shown in the present work highlight the following points:

- the present one-dimensional model can provide three-dimensional results in the case of thermo-piezo-elastic analysis;
- the present model can deal with the analysis of layered structures with piezo-patches;
- both sensor and actuator patches can be considered;
- the computational costs can be reduced whit respect to full three-dimensional models.

In short the present formulation can be considered a valid option for the multi-field analysis analysis of layered structures.

References

1. Ahmad, S.N., Upadhyay, C.S., Venkatesan, C.: Electro-thermo-elastic formulation for the analysis of smart structures. Smart Materials and Structures **15**(2), 401 (2006)

2. Ambrosini, R.: A modified Vlasov theory for dynamic analysis of thin-walled and variable open section beams. Engineering Structures **22**(8), 890–900 (2000). DOI 10.1016/S0141-0296(99)00043-7
3. Bailey, T., Hubbard, J.: Distributed piezoelectric polymer active vibration control of a cantilever beam. AIAA Journal **8**, 605–611 (1985)
4. Benjeddou, A., Trindade, M., Ohayon, R.: A unified beam finite element model for extension and shear piezoelectric actuation mechanisms. Journal of Intelligent Material Systems and Structures **8**(12), 1012–1025 (1997)
5. Berdichevsky, V.L.: Equations of the theory of anisotropic inhomogeneous rods. Dokl. Akad. Nauk **228**, 558–561 (1976)
6. Biscani, F., Nali, P., Belouettar, S., Carrera, E.: Coupling of hierarchical piezoelectric plate finite elements via arlequin method. Journal of intelligent materials systems and structures **23**, 749 (2012)
7. Carrera, E.: C_z^0 Requirements – Models for the two dimensional analysis of multilayered structures. Composite Structure **37**, 373–384 (1997)
8. Carrera, E.: An improved reissner-mindlin-type model for the electromechanical analysis of multilayered plates including piezo-layers. Journal of Intelligent Material Systems and Structures **8**, 232–248 (1997)
9. Carrera, E.: An assessment of mixed and classical theories for thermal stress analysis of orthotropic multilayered plates. Journal of Thermal Stresses **23**, 797–831 (2000)
10. Carrera, E.: Theories and finite elements for multilayered plates and shells: A unified compact formulation with numerical assessment and benchmarking. Archives of Computational Methods in Engineering **10**, 215–297 (2003)
11. Carrera, E., Boscolo, M.: Hierarchic multilayered plate elements for coupled multifield problems of piezoelectric adaptive structures: Formulation and numerical assessment. Archives of Computational Methods in Engineering **14**(4), 383–430 (2007)
12. Carrera, E., Boscolo, M., Robaldo, A.: Hierarchic multilayered plate elements for coupled multifield problems of piezoelectric adaptive structures: Formulation and numerical assessment. Archives of Computational Methods in Engineering **14**(4), 383–430 (2007)
13. Carrera, E., Brischetto, S., Nali, P.: Variational Statements and Computational Models for MultiField Problems and Multilayered Structures. Mechanics of Advanced Materials and Structures **15**(3-4), 182–198 (2008). DOI 10.1080/15376490801907657
14. Carrera, E., Cinefra, M., Petrolo, M., Zappino, E.: Comparisons between 1d (beam) and 2d (plate/shell) finite elements to analyze thin walled structures. Aerotecnica Misssili & Spazio. The journal of Aerospace Science, Technology and Systems **93**(1-2) (2014)
15. Carrera, E., Cinefra, M., Petrolo, M., Zappino, E.: Finite Element Analysis of Structures Through Unified Formulation. John Wiley & Sons (2014)
16. Carrera, E., Filippi, M., Zappino, E., Carrera E., F.M., E.., Z., Carrera, E., Filippi, M., Zappino, E.: Free vibration analysis of laminated beam by polynomial, trigonometric, exponential and zig-zag theories. Journal of Composite Materials **48**(19), 2299–2316 (2014). DOI 10.1177/0021998313497775
17. Carrera, E., Gaetano, G., M., P.: Beam Structures, Classical and Advanced Theories. John Wiley & Sons (2011)
18. Carrera, E., Giunta, G., Nali, P., Petrolo, M.: Refined beam elements with arbitrary crpss-section geometries. Computers and Structures **88**, 283–293 (2010)
19. Carrera, E., Petrolo, M.: Refined beam elements with only displacement variables and plate/shell capabilities. Meccanica **47**, 537–556 (2012)
20. Carrera, E., Petrolo, M., Nali, P.: Unified formulation applied to free vibrations finite element analysis of beams with arbitrary section. Shock and vibrations **18**(3), 485–502 (2011)
21. Carrera, E., Petrolo, M., Varello, A.: Advanced beam formulations for free vibrations analysis of conventional and joined wings. Journal of aerospace engineering **25**(2), 282–293 (2012)
22. Carrera, E., Robaldo, A.: Extension of reissner mixed variational principle to thermopiezelasticity. Atti della Accademia delle Scienze di Torino. Classe di Scienze Fisiche Matematiche e Naturali **31**, 27–42 (2007)

23. Carrera, E., Zappino, E., Petrolo, M.: Advanced elements for the static analysis of beams with compact and bridge-like sections. Journal of structural engineering **56**, 49–61 (2012)
24. Caruso, G., Galeani, S., Menini, L.: Active vibration control of an elastic plate using multiple piezoelectric sensors and actuators. Simulation modelling prectice and theory **11**, 403–419 (2003)
25. Cowper, G.R.: The Shear Coefficient in Timoshenko's Beam Theory, volume = 33, year = 1966. Journal of Applied Mechanics (2), 335–340
26. Crawley, E., Luis, J.: Use of piezoelectric actuators as elements of intelligent structures. AIAA Journal **25**, 1373–1385 (1987)
27. Davies, J.M., Leach, P.: First-order generalised beam theory. Journal of Constructional Steel Research **31**(2-3), 187–220 (1994)
28. Davies, J.M., Leach, P., Heinz, D.: Second-order generalised beam theory. Journal of Constructional Steel Research **31**(2-3), 221–241 (1994)
29. Dong, S.B., Alpdogan, C., Taciroglu, E.: Much ado about shear correction factors in Timoshenko beam theory. International Journal of Solids and Structures **47**(13), 1651–1665 (2010). DOI 10.1016/j.ijsolstr.2010.02.018
30. Dong, X.J., Meng, G., Peng, J.C.: Vibration control of piezoelectric actuators smart structures based on system identification technique. Journal of sound and vibration **297**, 680–693 (2006)
31. Euler, L.: De curvis elasticis. Methodus inveniendi lineas curvas maximi minimive proprietate gaudentes, sive solutio problematis iso-perimetrici lattissimo sensu accepti. (1744)
32. Friberg, P.O.: Beam element matrices derived from Vlasov's theory of open thin-walled elastic beams. International Journal for Numerical Methods in Engineering **21**, 1205–1228 (1985)
33. Giavotto, V., Borri, M., Mantegazza, P., Ghiringhelli, G., Carmaschi, V., Maffioli, G.C., Mussi, F.: Anisotropic beam theory and applications. Computers & Structures **16**(1), 403–413 (1983). DOI http://dx.doi.org/10.1016/0045-7949(83)90179-7
34. Kim, J., Varadan, V.V., Varadan, V.K.: Finite element modelling of structures including piezoelectric active devices. International journal for numerical methods in engineering **832**, 817–832 (1997)
35. Kim, T.W., Kim, J.H.: Optimal distribution of an active layer for transient vibration control of an flexible plates. Smart Material and Structures **14**, 904–916 (2005)
36. Kpeky, F., Abed-Meraim, F., Boudaoud, H., Daya, E.M.: Linear and quadratic solid–shell finite elements shb8pse and shb20e for the modeling of piezoelectric sandwich structures. Mechanics of Advanced Materials and Structures pp. 1–20 (2017)
37. Kumar, K., Narayanan, S.: The optimal location of piezolectric actuators and sensors for vibration controls of plate. Smart Material and Structures **16**, 2680–2691 (2007)
38. Kusculuoglu, Z.K., Royston, T.J.: Finite element formulation for composite plates with piezoceramic layers for optimal vibration control applications. Smart Material and Structures **14**, 1139–1153 (2005)
39. Liu, G., Dai, K., Lim, K.: Static and vibration control of composite laminates integrated with piezoelectric sensors and actuators using radial point interpolation method. Smart Material and Structures **14**, 1438–1447 (2004)
40. Miglioretti, F., Carrera, E., Petrolo, M.: Variable kinematic beam elements for electromechanical analysis. Smart Structures and Systems **13**(4), 517–546 (2014)
41. Moita, J., Soares, C., Soares, C.: Active control of forced vibration in adaptive structures using a higher order model. Composite Structures **71**, 349–355 (2005)
42. Moitha, J., Correira, I., Soares, C., Soares, C.: Active control of adaptive laminated structures with bonded piezoelectric sensors and actuators. Computer and Structures **82**, 1349–1358 (2004)
43. Robaldo, A., Carrera, E., Benjeddou, A.: Unified formulation for finite element thermoleastic analysis of multilayered anisotropic composite plates. Journal of Thermal Stresses **28**, 1031–1064 (2005)
44. Robaldo, A., Carrera, E., Benjeddou, A.: A unified formulation for finite element analysis of piezoelectric plates. Computers & Structures **84**, 1494–1505 (2006)

45. de Saint-Venant, A.: Mémoire sur la Torsion des Prismes, avec des considérations sur leur flexion, ainsi que sur l'équilibre interieur des solides élastiques en général, et des formules pratiques pour le calcul de leur résistance à divers efforts s'exerçant simultanément. Académie des Sciences de l'Institut Impérial de Frances **14**, 233–560 (1856)
46. Sarvanos, D., Heyliger, P.: Mechanics and computational models for laminated piezoelectric beams, plate, and shells. Applied mechanic review **52**(10), 305–320 (1999)
47. Schardt, R.: Eine Erweiterung der Technischen Biegetheorie zur Berech- nung Prismatischer Faltwerke. Der Stahlbau **35**, 161–171 (1966)
48. Silvestre, N., Silvestre N., Camotim, D., Silvestre, N., Camotim, D., Silvestre N., Camotim, D., Silvestre, N., Camotim, D.: First-Order Generalised Beam Theory for Arbitrary Orthotropic Materials. Thin-Walled Structures **40**(9), 791–820 (2002). DOI 10.1016/S0263-8231(02)00026-5
49. Sun, C., Zhang, X.: Use of thickness-shear mode in adaptive sandwich structures. Smart Materials and Structures **4**(3), 202 (1995)
50. Timoshenko, S.P.: On the corrections for shear of the differential equation for transverse vibrations of prismatic bars. Philosophical Magazine **41**, 744–746 (1921)
51. Tzou, H.S., Ye, R.: Piezothermoelasticity and precision control of piezoelectric systems: Theory and finite element analysis. Journal of Vibration and Acoustics **116**(4), 489–495 (1994)
52. Vasques, C., Rodrigues, J.: Active vibration of smart piezoelectric beams: comparison of classical and optimal feedback control strategies. Computer and Structures **84**, 1459–1470 (2006)
53. Vidal, P., D'Ottavio, M., Thaier, M., Polit, O.: An efficient finite shell element for the static resposne of piezoelectric laminates. Journal of intelligent materials systems and structures **22**, 671 (2011)
54. Vlasov, V.Z.: Thin walled elastic beams (1961)
55. Volovoi, V.V.: Asymptotic theory for static behavior of elastic anisotropic I-beams. International Journal of Solids and Structures **36**(7), 1017–1043 (1999). DOI 10.1016/S0020-7683(97)00341-7
56. Washizu, K.: Variational methods in elasticity and plasticity. Oxford: Pergamon Press (1968)
57. Xu, S., Koko, T.: Finite element analysis and design of actively acontrolled piezoelectric smart structure. Finite element in Analysis and Design **40**, 241–262 (2004)
58. Yu, W., Hodges, D.H.: Elasticity Solutions Versus Asymptotic Sectional Analysis of Homogeneous, Isotropic, Prismatic Beams. Journal of Applied Mechanics **71**(1), 15 (2004). DOI 10.1115/1.1640367
59. Yu, W., Volovoi, V.V., Hodges, D.H., Hong, X.: Validation of the variational asymptotic beam sectional analysis (VABS). AIAA Journal **40**, 2105–2113 (2002)
60. Zappino, E., Carrera, E., Rowe, S., Mangeot, C., Marques, H.: Numerical analyses of piezoceramic actuators for high temperature applications. Composite Structures **151**, 36 – 46 (2016). DOI http://dx.doi.org/10.1016/j.compstruct.2016.01.084. Smart composites and composite structures In honour of the 70th anniversary of Professor Carlos Alberto Mota Soares
61. Zhang, X., Sun, C.: Formulation of an adaptive sandwich beam. Smart Materials and Structures **5**(6), 814 (1996)
62. Zhang, X.D., Sun, C.T.: Formulation of an adaptive sandwich beam. Smart Materials and Structures **5**(6), 814 (1996)
63. Zhou, X., Chattopadhyay, A., Gu, H.: Dynamic resposne of smart composites using a coupled thermo-piezoelectric-mechanical model. AIAA Journal **38**, 1939–1948 (2000)
64. Zhou, Y.S., Tiersten, H.F.: An elastic analysis of laminated composite plates in cylindrical bending due to piezoelectric actuators. Smart Materials and Structures **3**(3), 255 (1994)